DOI: 10.1002/ejic.200601255

Unraveling the *o*-Methoxy Effect in the CO/Ethene Copolymerization Reaction by Diphosphanepalladium(II) Catalysis

Claudio Bianchini,*[a] Andrea Meli,[a] Werner Oberhauser,*[a] Carmen Claver,[b] and Eduardo J. Garcia Suarez[b]

Keywords: Polyketones / Palladium / Diphosphane ligands / Catalysis / Copolymerization / Kinetics

Relevant steps in the CO/ethene copolymerization reaction, namely the migratory insertion of $[Pd(Me)(CO)(P\text{-}P)]BAr'_4$ and the carbonylation of the β-keto chelates $[Pd(CH_2CH_2C(O)Me)(P\text{-}P)]BAr'_4$ have been studied by in situ high-pressure NMR spectroscopy in CH_2Cl_2; P-P = 1,2-bis[bis(2-methoxyphenyl)phosphanyl]ethane or 1,3-bis[bis(2-methoxyphenyl)phosphanyl]propane. This study, backed by batch catalytic reactions in the same solvent, has contributed to rationalizing the higher catalytic activity of Pd^{II} catalysts modified with *o*-methoxy-substituted diphosphane ligands as compared to analogous Pd^{II} catalysts with 1,2-bis(diphenylphosphanyl)ethane (dppe) and 1,3-bis(diphenylphosphanyl)propane (dppp) ligands. It was found that *o*-MeO substituents on the phosphorus aryl rings ease the opening of the β-chelate ring by CO and affect the kinetics of the overall CO/ethene copolymerization. Indeed, unlike the catalysts with the dppe and dppp ligands, the rate of carbonylation of the *o*-MeO-modified β-keto chelates is limited by the Pd(alkyl)(CO) migratory insertion, which makes the overall copolymerization process independent of the CO pressure.

Introduction

Perfectly alternating polyketones are high-performance thermoplastics obtainable by copolymerization of carbon monoxide and alkenes, generally ethene, in the presence of Pd^{II} catalysts modified with chelating diphosphanes (Scheme 1).[1] The copolymerization reactions are commonly performed in protic solvents (alcohols, preferentially methanol), yet aprotic solvents such as CH_2Cl_2 are used in reactions catalyzed by Pd^{II} alkyl precursors as well as in model mechanistic studies.[2]

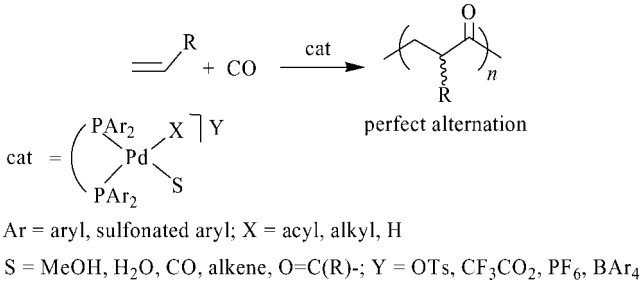

Scheme 1. Copolymerization reaction with $Pd^{II}(P\text{-}P)$ complexes.

The introduction of one *o*-methoxy substituent on each phosphorus aryl ring of the ligand greatly enhances the productivity as compared to reactions promoted by catalysts with unsubstituted diphosphanes.[2d,3]

Both steric and electronic factors have been invoked to account for the positive effect of the *o*-methoxy groups on the catalyst activity, yet no clear-cut explanation has been put forward so far. Indeed, most of the previous hypotheses are based on indirect observations such as the decreased formation of catalytically inactive bis-chelates or binuclear species;[4] the reduced tendency towards phosphane oxidation;[5a] the increased basicity of the metal center;[5b] and the reduced stability of catalyst resting states.[5c]

Intrigued by the possibility of elucidating the *ortho-methoxy effect*, we decided to look at two well-known reactions occurring during the propagation step of the alternating CO/C_2H_4 copolymerization: (i) the migratory insertion of $[Pd(Me)(CO)(P\text{-}P)]^+$ complexes and (ii) the carbonylation of the β-keto chelates $[Pd(CH_2CH_2C(O)Me)(P\text{-}P)]^+$ (Scheme 2).[5b,5c]

To this purpose, complexes stabilized by the two couples of ligands shown in Scheme 3 were employed as model compounds.[5b,5c]

In situ high-pressure NMR (HPNMR) and IR techniques have been employed to determine kinetic and thermodynamic parameters, while batch catalytic reactions under different experimental conditions have provided information on the dependence of the reaction rate on CO and ethene pressures. Incorporation of the results obtained

[a] Istituto di Chimica dei Composti Organometallici (ICCOM-CNR), Area di Ricerca CNR di Firenze,
Via Madonna del Piano 10, 50019 Sesto Fiorentino, Italy
Fax: +39-0555225203
E-mail: claudio.bianchini@iccom.cnr.it
werner.oberhauser@iccom.cnr.it
[b] Dept. De Quìmica Fìsica i Inorganica, Facultat de Quìmica, Universitat Rovira i Virgili,
c/Marcel.li Domingo s/n, 43007 Tarragona, Spain

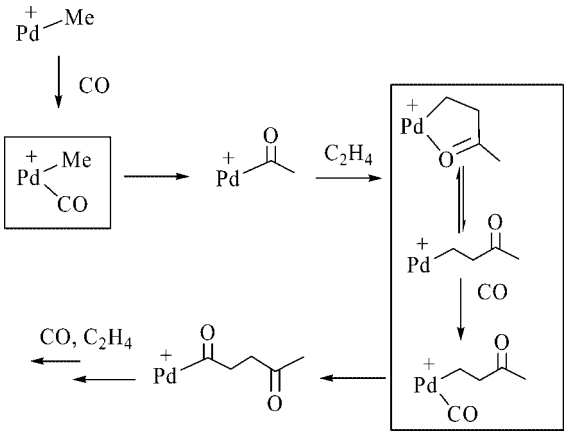

Scheme 2.

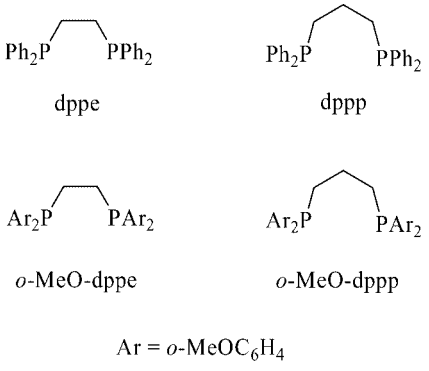

Scheme 3.

unambiguously show that the *o*-methoxy groups can interact with the metal center, leading to a mechanism where the opening of the β-keto chelates and the overall copolymerization rate as well are zero-order with respect to the CO pressure.

Results and Discussion

Generation of the β-Keto Chelates [Pd($CH_2CH_2C(O)Me$)(P-P)]BAr'_4

The synthetic procedure for the β-keto chelate complexes [Pd($CH_2CH_2C(O)Me$)(P-P)]BAr'_4 (P-P = *o*-MeO-dppe, **3c**; *o*-MeO-dppp, **4c**; Ar′ = 3,5-$(CF_3)_2$-C_6H_3) is illustrated in Scheme 4.

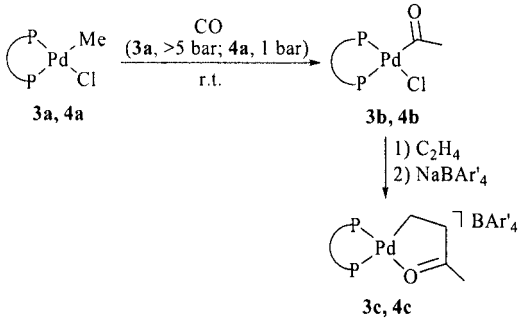

Scheme 4. In situ synthesis of the Pd^{II} β-keto chelates **3c** and **4c**.

The chlorido-methyl precursors [PdCl(Me)(P-P)] (P-P = *o*-MeO-dppe, **3a**; *o*-MeO-dppp, **4a**) were conveniently prepared by the plain reaction of PdCl(Me)(COD) (COD = cycloocta-1,5-diene) with the appropriate diphosphane and isolated as off-white crystalline solids in 78 and 67% yield, respectively.[2d] Unambiguous characterization of **3a** and **4a** in solution was achieved by variable-temperature ^1H and $^{31}P\{^1H\}$ NMR spectroscopy in CD_2Cl_2. Complexes **3a** and **4a** exhibit fluxional behavior on the NMR time-scale due to the exchange of equatorial and axial aryl groups. The ^1H NMR spectrum at 21 °C of either complex displayed one set of resonances for the aryl hydrogen atoms (δ = 6.87–7.91 and 6.87–7.58 ppm, respectively) and two singlets for the methoxy groups (δ = 3.59/3.60 and 3.66/3.76 ppm, respectively), which is consistent with the presence of two couples of equivalent aryl groups in the *o*-MeO-ligands. Decreasing the temperature led to a progressive broadening of all resonances. At –70 °C, the ^1H NMR spectra of **3a** and **4a** showed four singlets for the methoxy groups at δ = 3.42, 3.44, 3.75, and 3.76 ppm and δ = 3.56, 3.67, 3.69, and 3.72 ppm, respectively. This pattern can be safely attributed to the formation of equatorially and axially oriented methoxy groups as illustrated in the sketch reported in Scheme 5.[2d,6]

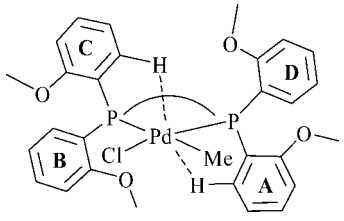

Scheme 5. Low temperature conformation of **3a** and **4a**.

The ^1H NMR spectra at –70 °C showed also a significant downfield shift of the resonances of two aryl hydrogen atoms (δ = 8.45/8.61 and 8.55/8.74 ppm, respectively), which, on the basis of ^1H-^{31}P COSY experiments, can be assigned to the *o*-H atoms of the axial aryl rings **A** and **C** interacting with the metal center. Analogous fluxional behavior has been previously reported for the X-ray authenticated complexes $PdCl_2$(P-P) (P-P = *o*-MeO-dppe, *o*-MeO-dppp).[2d] Further spectroscopic evidence in support of the conformation proposed in Scheme 5 was provided by a ^1H ROESY experiment at –70 °C of **3a**, indicating two significant correlations between the hydrogen atoms of the Pd methyl group and the *o*-H atoms of the aryl rings **A** and **C**.

A single-crystal X-ray analysis of **3a**·$CHCl_3$ has confirmed the structure proposed in solution. Suitable crystals were obtained by slow diffusion of toluene into a $CHCl_3$ solution of **3a**. An ORTEP drawing of **3a**·$CHCl_3$ is shown in Figure 1, while selected distances and angles are reported in Table 1.

The crystal structure shows a square-planar palladium center coordinated by *cis* phosphorus atoms. The Pd–P bond lengths of 2.221(2) Å (*trans* to chloride) and 2.343(2) Å (*trans* to methyl) are in line with the greater *trans*-influence of the methyl group as compared to chlo-

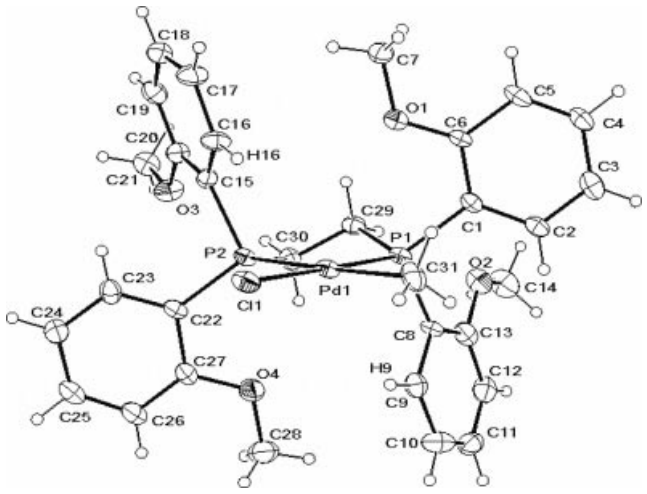

Figure 1. ORTEP plot of **3a**·$CHCl_3$. The solvent molecule was omitted for clarity. Thermal ellipsoids are shown at the 30% probability level.

Table 1. Selected bond lengths and bond angles for **3a·CHCl$_3$**.

Bond lengths [Å] and bond angles [°]	
Pd(1)–P(1)	2.221(2)
Pd(1)–P(2)	2.343(2)
Pd(1)–Cl(1)	2.389(2)
Pd(1)–C(31)	2.095(8)
P(1)–Pd(1)–P(2)	86.27(9)
C(31)–Pd(1)–Cl(1)	89.30(20)
Intramolecular distances [Å]	
Pd(1)–O(1)	3.573(6)
Pd(1)–O(2)	5.181(6)
Pd(1)–O(3)	5.271(7)
Pd(1)–O(4)	3.870(6)
Pd(1)–H(9)	2.809
Pd(1)–H(16)	2.855

ride. The four *o*-methoxy oxygen atoms are disposed around the palladium center in such a way that two of them, O(1) and O(4), point to the metal center occupying a pseudo-apical position (Pd···O distances of 3.573(6) and 3.870(6) Å], while the other two, O(2) and O(3), are close to pseudo-equatorial positions (Pd···O distances of 5.181(6) and 5.271(7) Å]. All of these Pd···O distances are too large for an effective electrostatic interaction between palladium and the *o*-methoxy groups. In contrast, the *o*-H atoms H(9) and H(16) show short intramolecular Pd···H distances of 2.809 and 2.855 Å, respectively, which are comparable to those found in the crystal structure of $PdCl_2$(*o*-MeO-dppe).[2d]

Pressurizing a CH_2Cl_2 solution of **3a** with >5 bar CO in a 10-mm-OD HPNMR tube at room temperature led to the immediate formation of the acetyl complex PdCl(COMe)(*o*-MeO-dppe) (**3b**). In contrast, the formation of the complex PdCl(COMe)(*o*-MeO-dppp) (**4b**) from **4a** required no pressurization as it was quantitatively obtained by bubbling CO into a CH_2Cl_2 solution of the methyl complex at room temperature (Scheme 4). Once formed, the acetyl complexes were stable in solution even in the absence of CO.

Ethene bubbling into CH_2Cl_2 solutions of the acyl complexes **3b** and **4b** for 2 min, followed by the addition of stoichiometric $NaBAr'_4$, gave the β-keto chelates **3c** and **4c** (Scheme 4). Compounds **3b**, **3c**, **4b**, and **4c** have been unambiguously characterized by variable-temperature $^{31}P\{^1H\}$ and ^1H NMR spectroscopy. Selected NMR spectroscopic data are reported in Table 2 and Table 3, respectively.

Like the chlorido-methyl precursors **3a** and **4a**, the β-keto chelates **3c** and **4c** exhibit fluxional behavior in CD_2Cl_2 solution at room temperature, due to the exchange of equatorial and axial aryl groups. At –70 °C both compounds adopt the conformation shown in Scheme 6.

The ^1H NMR spectra of **3c** and **4c** at –70 °C showed a multiplet at δ = 8.48 and 8.28 ppm, respectively, which, on the basis of ^1H-^{31}P COSY experiments, was assigned to the

Table 2. $^{31}P\{^1H\}$ NMR chemical shifts in ppm, multiplicities in parentheses, and PP coupling constants (Hz) in square brackets for the palladium complexes $[Pd(X)(Y)(P\text{-}P)]^{0/+}$ in CD_2Cl_2 solutions at temperatures (°C) given in curly brackets.

P-P	X = COMe Y = Cl	X, Y = $(CH_2)_2$COMe	X = $(CH_2)_2$COMe Y = CO	X = $CO(CH_2)_2$COMe Y = CO
o-MeO-dppe	37.50 (d) [48.7] 27.80 (d) {22}	58.00 (d) [26.0] 26.77 (d) {–50}	57.55 (d) [29.5] 25.80 (d) {–50}	36.02 (d) [49.6] 16.74 (d) {–30}
o-MeO-dppp	15.40 (d) [75.9] –3.20 (d) {22}	33.90 (d) [57.6] –12.00 (br. s) {–90}	21.30 (d) [67.1] –30.50 (br. s) {–90}	8.86 (d) [86.9] –29.16 (d) {–30}

Table 3. ^1H NMR chemical shifts in ppm, multiplicities in parentheses, for the palladium complexes $[Pd(X)(Y)(P\text{-}P)]^{0/+}$ in CD_2Cl_2 solutions at temperatures (°C) given in curly brackets.

P-P	X = COMe Y = Cl	X, Y = $(CH_2)_2$COMe	X = $(CH_2)_2$COMe Y = CO	X = $CO(CH_2)_2$COMe Y = CO
o-MeO-dppe	1.79 (s) CO*Me* {22}	0.82 (br. m) PdCH_2 2.40 (s) CO*Me* 3.13 (m) CH_2COMe {–50}	0.30 (br. m) PdCH_2 2.10 (s) CO*Me* 2.65 (m) CH_2COMe {–50}	1.88 (s) CO*Me* 3.10 (m) CH_2COMe 2.25 (m) PdCOCH_2 {–30}
o-MeO-dppp	1.73 (s) CO*Me* {22}	0.84 (br. m) PdCH_2 2.17 (s) CO*Me* 2.89 (m) CH_2COMe {–90}	0.37 (br. m) PdCH_2 1.51 (s) CO*Me* 2.42 (m) CH_2COMe {–90}	1.92 (s) CO*Me* 2.52 (m) CH_2COMe 2.08 (m) PdCOCH_2 {–30}

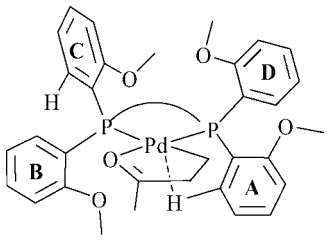

Scheme 6. Low temperature conformation of **3c** and **4c**.

o-H atom of ring **A**. At the same temperature, a ^{1}H-ROESY experiment of **3c** revealed the existence of significant correlations between the Pd-CH_2 unit and the *o*-H atoms of the aryl rings **A** and **D** and between the *o*-methoxy hydrogen atoms from the equatorial aryl ring **B** and the hydrogen atoms of the COMe unit. The stereochemical position of the aryl ring **C** could not be unambiguously determined, yet, due to the lack of the downfield-shifted multiplet of the *o*-H atom of ring **C** in the ^{1}H NMR spectrum, it is likely that ring **C** is turned around in such a way that the corresponding *o*-methoxy group points towards the metal center.

The β-keto chelates **3c** and **4c** and the corresponding derivatives with dppe (**1c**) and dppp (**2c**) were also characterized by in-situ IR spectroscopy in CH_2Cl_2 at room temperature (Table 4). The spectra were scarcely informative except for showing a blue shift of ca. 6 cm^{-1} of the C=O stretching band for the *o*-methoxy-susbstituted complexes, which is consistent with the higher σ-donor ability of *o*-MeO-dppe and *o*-MeO-dppp as compared to dppe and dppp.

Table 4. Selected IR absorption bands in CH_2Cl_2 of selected complexes.

	[Pd(CH_2CH_2C(O)Me)-(P-P)]BAr′$_4$ ν(C=O) [cm^{-1}]	[Pd(CO)(COMe)-(P-P)]BAr′$_4$ ν(CO)/ν(C=O) [cm^{-1}]
o-MeO-dppe	1636	2122/1696
dppe	1629	2130/1693
o-MeO-dppp	1636	2122/1700
dppp	1630	2129/1694

Generation and Migratory Insertion Barriers of [PdMe(CO)(P-P)]BAr′$_4$

The carbonyl-methyl complexes [PdMe(CO)(P-P)]BAr′$_4$ (P-P = *o*-MeO-dppe, **3d**; *o*-MeO-dppp, **4d**) were selectively generated in situ by bubbling CO into a HPNMR tube containing a CD_2Cl_2 solution of the corresponding chloridomethyl complex at –120 °C.

The kinetics of conversion of the carbonyl-methyl complexes to the (acetyl)carbonyl products [Pd(CO)(COMe)-(P-P)]BAr′$_4$ (P-P = *o*-MeO-dppe, **3e**; *o*-MeO-dppp, **4e**) (Scheme 7) were conveniently followed by variable-temperature $^{31}P\{^1H\}$ NMR spectroscopy in CD_2Cl_2. $^{31}P\{^1H\}$ and ^{1}H NMR spectroscopic data for **3d**–**4e** are given in Table 5 and Table 6, respectively.

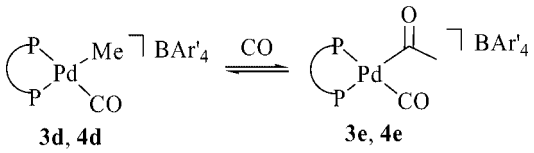

Scheme 7. Migratory insertion of **3d** and **4d**.

Table 5. $^{31}P\{^1H\}$ NMR chemical shifts in ppm, multiplicities in parentheses, and PP coupling constants (Hz) in square brackets for the palladium complexes [Pd(X)(Y)(P-P)]BAr′$_4$ in CD_2Cl_2 solutions at temperatures (°C) given in curly brackets.

P-P	X = Me,Y = CO	X = COMe, Y = CO
o-MeO-dppe	57.59 (d) [31.0]	35.75 (d) [48.7]
	24.34 (d) {–50}	16.55 (d) {–40}
o-MeO-dppp	22.40 (d) [62.8]	8.00 (d) [88.7]
	–29.9 (br. s) {–90}	–28.5 (d) {–40}

Table 6. ^{1}H NMR chemical shifts in ppm and multiplicities in parentheses for the palladium complexes [Pd(X)(Y)(P-P)]BAr′$_4$ in CD_2Cl_2 solutions at temperatures (°C) given in curly brackets.

P-P	X = Me, Y = CO	X = COMe, Y = CO
o-MeO-dppe	0.43 (m) {–50}	1.65 (s) {–40}
o-MeO-dppp	0.08 (m) {–90}	1.88 (s) {–40}

Consistent with the greater σ-donor ability of *o*-MeO-dppe and *o*-MeO-dppp vs. dppe and dppp, the IR spectra of the (acetyl)carbonyl complexes **3e** and **4e** in CH_2Cl_2 (Table 4) showed a blue shift of the COMe absorption band (3–6 cm^{-1}) and a red shift of the CO absorption band (7–8 cm^{-1}) as compared to the analogue derivatives [Pd(CO)-(COMe)(P-P)]BAr′$_4$ with dppe (**1e**) and dppp (**2e**).[2b,2c]

The study of the migratory insertion of the methyl(carbonyl) complexes was carried out at different CO pressures (5–20 bar), showing the reaction rate to be independent of the CO concentration. According to first-order kinetics, the free energy of activation for the migration insertion process was calculated applying the equation: $\Delta G^{\ddagger} = RT(\ln kT/h -$

Table 7. Experimental activation barriers and temperatures for the migratory insertions of (alkyl)carbonyl complexes and for the carbonylation of β-chelates.

P-P	[Pd(Me)(CO)(P-P)]$^+$			[Pd(CH_2CH_2C(O)Me)(P-P)]$^+$			[Pd(CH_2CH_2C(O)Me)(CO)(P-P)]$^+$		
	T [°C]	$t_{1/2}$ [min]	$\Delta G^{\ddagger}$ [kcal/mol]	T [°C]	$t_{1/2}$ [min]	p(CO) [bar]	T [°C]	$t_{1/2}$ [min]	$\Delta G^{\ddagger}$ [kcal/mol]
o-MeO-dppe	–40	52	17.4(1)	–60	25	20	–40	100	17.7(1)
dppe[2b]	–40	12	16.9(1)	–20	15	20			
o-MeO-dppp	–80	105	14.6(1)	–90	6	20	–60	10	15.2(1)
dppp[2c]	–60	10	15.2(1)	–70	84	20			

$\ln k_r$) with $k_r = \ln 2/t_{1/2}$ (T = temperature during the conversion; $t_{1/2}$ = half-life time in seconds).[2b,2c] The values of the activation energies for the migratory insertion in **3d** and **4d** are given in Table 7 that also reports data previously reported for the dppe and dppp analogues [PdMe(CO)(P-P)]-BAr'_4 (P-P = dppe, **1d**; dppp, **2d**).[2b,2c]

The results obtained showed the migratory insertion of PdMe(CO) to be a low-energy process for all complexes; in addition it was lower for the dppp complexes than for the dppe ones and, in particular, for the *o*-MeO-dppp complex **4d**, which is known to generate the most active catalysts in several reaction media.[2d]

Carbonylation Reactions of the β-Keto Chelates

The reactions of the β-keto chelates **3c** and **4c** with 20 bar CO in CD_2Cl_2 were studied in situ by ^1H and $^{31}P\{^1H\}$ HPNMR spectroscopy at low temperature. HPNMR tubes containing CD_2Cl_2 solutions of these complexes under nitrogen were cooled to ca. –120 °C, pressurized with 20 bar CO, and then inserted into the NMR probe-head pre-cooled to –90 °C. The conversion of the β-keto chelates into the (acyl)carbonyl complexes [Pd(CO)-$(COCH_2CH_2C(O)Me)$(P-P)]BAr'_4 (P-P = *o*-MeO-dppe, **3g**; *o*-MeO-dppp, **4g**) was found to involve (alkyl)carbonyl intermediates of the formula [Pd(CO)$(CH_2CH_2C(O)Me)$-(P-P)]BAr'_4 (P-P = *o*-MeO-dppe, **3f**; *o*-MeO-dppp, **4f**) (Scheme 8). Selected $^{31}P\{^1H\}$ and ^1H NMR spectroscopic data of the final products and intermediates are reported in Table 2 and Table 3, respectively, while sequences of $^{31}P\{^1H\}$ NMR spectra acquired during the carbonylation of either **3c** or **4c** with 20 bar CO are reported in Figure 2 and Figure 3, respectively.

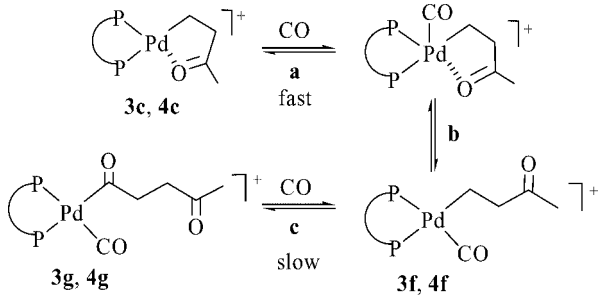

Scheme 8. Carbonylation of **3c** and **4c**.

Compound **3c** started to convert into the (alkyl)carbonyl complex **3f** at –60 °C with a $t_{1/2}$ value of 25 min (Figure 2, trace b). Increasing the temperature to –40° led to the quantitative formation of **3f** already after recording the first $^{31}P\{^1H\}$ NMR spectrum (trace c). At this temperature, **3f** slowly converted into the (acyl)carbonyl complex **3g** (trace d), which was the only phosphorus-containing species at room temperature (trace e).

In an analogous experiment, **4c** was found to convert already at –90 °C into the (alkyl)carbonyl complex **4f** (Figure 3, trace b), which, in turn, started to transform into the final (acyl)carbonyl product **4g** at –80 °C. Because of the slow conversion rate at this temperature, the migratory insertion of **4f** was more conveniently evaluated at –60 °C (trace d).

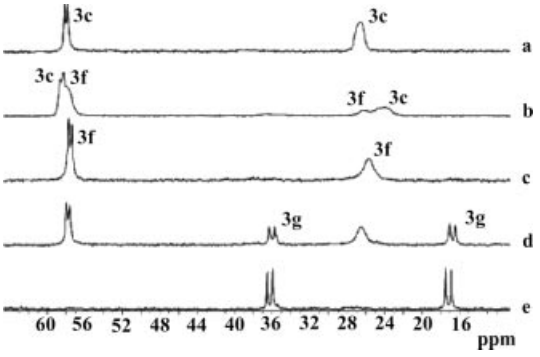

Figure 2. Variable-temperature $^{31}P\{^1H\}$ NMR study (sapphire tube, CD_2Cl_2, 81.01 MHz) of the carbonylation reaction of **3c**: (a) under nitrogen at –90 °C; (b) under CO (20 bar) after 40 min at –60 °C; (c) after 5 min at –40 °C; (d) after 80 min at –40 °C; (e) at room temperature.

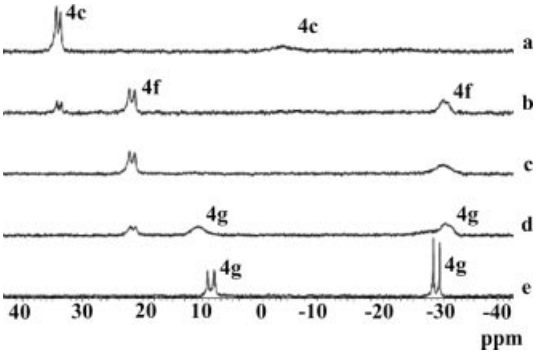

Figure 3. Variable-temperature $^{31}P\{^1H\}$ NMR study (sapphire tube, CD_2Cl_2, 81.01 MHz) of the carbonylation reaction of **4c**: (a) under nitrogen at –90 °C; (b) under CO (20 bar) after 30 min at –90 °C; (c) after 30 min at –80 °C; (d) after 10 min at –60 °C; (e) at room temperature.

To the best of our knowledge, (alkyl)carbonyl compounds such as **3f** and **4f** have never been intercepted along the carbonylation of diphosphane-modified palladium alkyl complexes. Like all the other new products obtained in situ, the characterization of the (alkyl)carbonyl complexes was achieved by NMR spectroscopy as well as by comparison with the spectra of similar or related complexes (i.e., γ-keto acyl chelates)[7] described in the literature (Table 2 and Table 3). Experimental evidence supporting the (alkyl)carbonyl structure of **3f** and **4f** was provided by the ^{31}P chemical shifts and the $^2J_{PP}$ coupling constants that were practically identical to those of the carbonyl-methyl complexes **3d** and **4d**. Moreover, the ^1H NMR shifts of the $PdCH_2CH_2C(O)Me$ units were significantly upfield shifted with respect to the values observed for the β-keto chelates (**3c** vs. **3f**: C(O)Me, δ = 2.40 vs. 2.10 ppm; $PdCH_2$, δ = 0.82 vs. 0.30 ppm; **4c** vs. **4f**: C(O)Me, δ = 2.17 vs. 1.51 ppm;

$PdCH_2$, δ = 0.84 vs. 0.37 ppm). In particular, the high-field shift of the C(O)Me singlets agrees well with the de-coordination of the carbonyl-oxygen atom from the metal center.[7g]

Temperatures and $t_{1/2}$ values for the conversion of the β-chelates **3c** and **4c** into the corresponding (alkyl)carbonyl product and the activation energies of the migratory insertions of the latter compounds are reported in Table 7. The opening of the β-chelate ring by CO is apparently easier for the *o*-MeO-susbstituted complexes than for the PPh_2-ones, which might well account for the greater catalytic activity of the former complexes in batch reactions.[2d,3–5]

In the light of the kinetic and thermodynamic data relative to the opening of the β-chelate ring by CO and to the alkyl migration to CO (Table 7), one may safely conclude that the latter process (step **c** of Scheme 8) limits the overall rate of the transformation of **3c** and **4c** into the (acyl)carbonyl products **3g** and **4g**, which is a relevant step in the propagation mechanism of the CO/ethene copolymerization by Pd^{II}-diphosphane catalysis.[1] Accordingly, since the Pd(CO)alkyl migratory insertion is independent of the CO pressure (vide infra), the overall copolymerization process would be independent of the CO pressure, at least under a gas pressure of 20 bar. This result dramatically differs from the previously reported studies of CO/ethene copolymerization by the PPh_2-precursors **1c** and **2c** where the actual copolymerization rate depends on both CO and C_2H_4 pressure[8] and the opening of the β-chelates by CO is the rate-limiting step in the propagation step involving CO insertion (Table 7).[2b,2c]

Catalytic CO/Ethene Copolymerization Reactions

In an attempt to determine the dependence of the copolymerization rate on CO and ethene pressures under actual catalytic conditions, several batch reactions were carried out using either the *o*-MeO-modified chlorido-methyl complex **4a** or the analogous dppp derivative **2a** in CH_2Cl_2 at 50 °C.[2d] The results of this study are summarized in Table 8 which also reports data obtained in MeOH with the known catalyst $[Pd(H_2O)_2(o\text{-MeO-dppp})](OTs)_2$ (**4h**).[2d] In excellent accord with the present kinetic study, the catalytic activity of **4a** did not vary with the CO pressure in the range from 5 to 30 bar (entries 1, 2, 4), whereas an increase in activity occurred on increasing the C_2H_4 pressure (entry 3 vs. 2). In contrast, the productivity of the dppp precursor **2a** showed a clear dependence on the CO pressure (entries 5–6), which is in agreement with a previous kinetic study by Toniolo and Chaudhary for reactions carried out in MeOH.[8] The latter solvent was therefore used in reactions catalyzed by the *o*-MeO-dppp precursor **4h** (entries 7–9) which showed no dependence on the CO pressure above 10 bar, thus confirming and generalizing the results of the present kinetic study in CH_2Cl_2. Noteworthy, a zero-order dependence on the CO pressure has also been reported for the CO/ethene/propene terpolymerization catalyzed by the water-soluble system Pd acetate/sulfonated *o*-MeO-dppp.[3d]

Table 8. Ethene/CO copolymerization reactions catalyzed by diphosphanepalladium precursors in different solvents.

Entry[a]	Precursor	P(CO) [bar]	$P(C_2H_4)$ [bar]	Productivity[b]
1	PdCl(Me)(*o*-MeO-dppp)	5	20	5.0
2	PdCl(Me)(*o*-MeO-dppp)	20	20	5.1
3	PdCl(Me)(*o*-MeO-dppp)	20	40	7.4
4	PdCl(Me)(*o*-MeO-dppp)	30	20	4.9
5	PdCl(Me)(dppp)	5	20	0.6
6	PdCl(Me)(dppp)	20	20	2.8
7[c]	$[Pd(H_2O)_2(o\text{-MeO-dppp})](OTs)_2$	10	20	17.0
8[c]	$[Pd(H_2O)_2(o\text{-MeO-dppp})](OTs)_2$	15	20	16.8
9[c]	$[Pd(H_2O)_2(o\text{-MeO-dppp})](OTs)_2$	20	20	18.1

[a] Reaction conditions: precursor (0.010 mmol), CH_2Cl_2 (75 mL), $NaBAr'_4$ (1.5 equiv.), BQ (80 equiv.), 20 min, 50 °C, 1200 rpm. [b] Productivity: kilograms of alt-E-CO (g Pd × h)$^{-1}$. [c] Reaction conditions: precursor (0.0024 mmol), MeOH (100 mL), 1 h, 85 °C, 1200 rpm.

Conclusions

The present study confirms that *o*-MeO substituents on the P-aryl rings of chelating diphosphanes exert a beneficial effect on the activity of Pd^{II} catalysts for the alternating CO/ethene copolymerization. Electronic effects, related to the ability of the methoxy oxygen atoms to interact with the metal center, seem to play a major role in driving the catalytic activity. Indeed, even though no direct evidence for the coordination of the *o*-MeO group to palladium has been observed in the course of either migratory insertion or carbonylation reactions, NMR spectroscopy has shown the aryl rings to adopt a conformation which favors the interaction between the *o*-MeO oxygen atoms and the metal center.

High-pressure NMR studies supported by batch catalytic reactions have unambiguously shown that the presence of *o*-MeO substituents on the P-aryl rings affects the kinetics of the CO/ethene copolymerization by Pd^{II}-chelating diphosphane catalysis. Unlike analogous catalysts without *o*-methoxy-substituted ligands, the rate of carbonylation of the β-keto chelates is limited by the Pd(alkyl)(CO) migratory insertion, which makes the overall copolymerization process independent of the CO pressure, at least in the range of the partial CO pressures investigated (5–30 bar).

Experimental Section

General Procedures: All reactions and manipulations were carried out under nitrogen using Schlenk-type techniques. The solvents were generally distilled from dehydrating reagents and were deoxygenated before use. The reagents were used as purchased from Aldrich or Fluka, unless stated otherwise. PdCl(Me)(COD)[9] (COD = cycloocta-1,5-diene), $[Pd(CH_2CH_2C(O)Me)(dppe)]BAr'_4$ (**1c**),[2b] $[Pd(CH_2CH_2C(O)Me)(dppp)]BAr'_4$ (**2c**),[2c] [Pd(CO)(C(O)Me)-(dppe)]BAr'_4 (**1e**),[2b] [Pd(CO)(C(O)Me)(dppp)]BAr'_4 (**2e**),[2c] and $NaBAr'_4$[10] were prepared according to literature methods. All the isolated solid samples were collected on sintered-glass frits and washed with appropriate solvents before being dried under a stream of nitrogen. Copolymerization reactions were performed with a 250-mL stainless steel autoclave, constructed at the ICCOM-CNR

(Florence, Italy), equipped with a magnetic drive stirrer and a Parr 4842 temperature and pressure controller. The autoclave was connected to a gas reservoir to maintain a constant pressure during the catalytic reactions. GC/MS analyses of the solutions were performed on a Shimadzu QP2100S apparatus equipped with a SPB-1 Supelco fused silica capillary column (30 m, 0.25 mm i.d., 0.25 μm film thickness). Deuterated solvents for routine NMR measurements were dried with molecular sieves. ^{1}H, $^{13}C\{^{1}H\}$, $^{31}P\{^{1}H\}$ NMR spectra were obtained with either a Bruker ACP 200 (200.13, 50.32 and 81.01 MHz, respectively) or a Bruker Avance DRX-400 spectrometer (400.13, 100.62 and 161.98 MHz), respectively. Chemical shifts are reported in ppm (δ) relative to TMS, referenced to the chemical shifts of residual solvent resonances (^{1}H and ^{13}C NMR) or 85% H_3PO_4 (^{31}P NMR). ^{1}H-^{31}P COSY spectra and ^{1}H ROESY were recorded with a Bruker Avance DRX-400 spectrometer. High-pressure NMR experiments were carried out on the Bruker ACP 200 using a 10-mm sapphire NMR tube, which was purchased from Saphikon (Milford, NH), while the titanium high-pressure charging head was constructed at the ISSECC-CNR (Florence, Italy).[11] Elemental analyses were performed using a Carlo Erba Model 1106 elemental analyzer. Infrared spectra were recorded on a FT-IR Spectrum GX instrument (Perkin–Elmer).

***S*ynthesis of the Methyl-chlorido Complexes PdCl(Me)(P-P):**[2d] A solid sample of PdCl(Me)(COD) (0.20 mmol, 52.99 mg) was added to a stirred solution of the appropriate diphosphane ligand (0.20 mmol) in CH_2Cl_2 (20 mL) at room temperature. After 1 h, the resulting colorless solution was concentrated to ca. 5 mL under reduced pressure. Addition of *n*-pentane/diethyl ether (1:1, v/v; 20 mL) led to the precipitation of [PdCl(Me)(P-P)] (P-P = *o*-MeO-dppe, **3a**; *o*-MeO-dppp, **4a**) as an off-white solid, which was filtered off, washed with *n*-pentane, and dried under a stream of nitrogen.

3a: Yield 78%, 105.31 mg. $C_{31}H_{35}ClO_4P_2Pd$ (675.11): calcd. C 55.13, H 5.22; found C 55.09, H 5.24. $^{31}P\{^{1}H\}$ NMR (81.1 MHz, $CDCl_3$, 21 °C): δ = 61.09 (d, $^{2}J_{P,P}$ = 22.0 Hz, P_A), 39.07 (d, P_M) ppm. ^{1}H NMR (200.13 MHz, $CDCl_3$, 21 °C): δ = 0.40 (dd, $^{3}J_{H,PM}$ = 8.0 Hz, $^{3}J_{H,PA}$ = 3.2 Hz, 3 H, PdMe), 2.19–2.93 (m, 4 H, PCH_2), 3.59 (s, 6 H, OMe), 3.60 (s, 6 H, OMe), 6.87–7.91 (m, 16 H, Ar) ppm. $^{31}P\{^{1}H\}$ NMR (161.98 MHz, CD_2Cl_2, –70 °C): δ = 60.70 (d, $^{2}J_{P,P}$ = 23.2 Hz, P_A), 38.32 (d, P_M) ppm. ^{1}H NMR (400.16 MHz, CD_2Cl_2, –70 °C): δ = 0.40 (dd, $^{3}J_{H,PM}$ = 8.0 Hz, $^{3}J_{H,PA}$ = 3.0 Hz, 3 H, PdMe), 2.08 (m, 1 H, PCH*H*), 2.38 (m, 1 H, P′CH*H*), 2.91 (dt, $^{2}J_{H,P}$ = 56.0 Hz, $^{3}J_{H,H}$ = 13.6 Hz, 1 H, PC*H*H), 3.08 (dt, $^{2}J_{H,P}$ = 56.0 Hz, $^{3}J_{H,H}$ = 13.6 Hz, 1 H, P′C*H*H), 3.42 (s, 3 H, OMe), 3.44 (s, 3 H, OMe), 3.76 (s, 6 H, OMe), 6.72–7.73 (m, 14 H, Ar), 8.45 (dd, $^{2}J_{H,P}$ = 15.9 Hz, $^{3}J_{H,H}$ = 7.3 Hz, 1 H, *o*-H-$Ar_{ax.}$(A), 8.61 (dd, $^{2}J_{H,P}$ = 15.1 Hz, $^{3}J_{H,H}$ = 7.5 Hz, 1 H, *o*-H-$Ar_{ax.}$(C)) ppm.

4a: Yield 67%, 91.92 mg. $C_{32}H_{37}ClO_4P_2Pd$ (689.11): calcd. C 55.75, H 5.41; found C 55.74, H 5.43. $^{31}P\{^{1}H\}$ NMR (81.01 MHz, $CDCl_3$, 21 °C): δ = 30.80 (d, $^{2}J_{P,P}$ = 52.5 Hz, P_A), –0.56 (d, P_M) ppm. ^{1}H NMR (200.13 MHz, $CDCl_3$, 21 °C): δ = 0.32 (dd, $^{3}J_{H,PM}$ = 7.9 Hz, $^{3}J_{H,PA}$ = 3.5 Hz, PdMe), 1.92 (m, 2 H, CH_2), 2.43 (m, 2 H, PCH_2), 2.57 (m, 2 H, PCH_2), 3.66 (s, 6 H, OMe), 3.75 (s, 3 H, OMe), 3.76 (s, 3 H, OMe), 6.87–7.58 (m, 16 H, Ar) ppm. $^{31}P\{^{1}H\}$ NMR (161.98 MHz, CD_2Cl_2, –70 °C): δ = 30.88 (d, $^{2}J_{P,P}$ = 51.4 Hz, P_A), –2.42 (d, P_M) ppm. ^{1}H NMR (400.16 MHz, CD_2Cl_2, –70 °C): δ = –0.89 (dd, $^{3}J_{H,PM}$ = 7.7 Hz, $^{3}J_{HPA}$ = 3.2 Hz, PdMe), 1.70 (m, 1 H, CH*H*)), 1.92 (m, 1 H, C*H*H), 2.20 (m, 1 H, PCH*H*), 2.30 (m, 1 H, P′CH*H*), 2.48 (m, 1 H, PC*H*H), 2.79 (m, 1 H, P′C*H*H), 3.56 (s, 3 H, OMe), 3.67 (s, 3 H, OMe), 3.69 (s, 3 H, OMe), 3.72 (s, 3 H, OMe), 6.67–7.71 (m, 14 H, Ar), 8.55 (dd, $^{2}J_{H,P}$ = 16.4 Hz, $^{3}J_{H,H}$ = 7.3 Hz, 1 H, *o*-H-$Ar_{ax.}$(A)), 8.74 (dd, $^{2}J_{H,P}$ = 14.7 Hz, $^{3}J_{H,H}$ = 7.1 Hz, 1 H, *o*-H-$Ar_{ax.}$(C)) ppm.

In Situ Synthesis of the (Acetyl)Chloride Complexes PdCl(COMe)-(P-P): In a typical experiment, a solid sample of the methyl-chlorido complex PdCl(Me)(P-P) (0.03 mmol) was dissolved in a Schlenk tube containing CD_2Cl_2 (2 mL) under nitrogen at room temperature. The resulting solution was first transferred into a 10-mm sapphire tube and then pressurized to >5 bar of CO at room temperature. Irrespective of the diphosphane the quantitative formation of the corresponding (acetyl)chloride complex PdCl(CO-Me)(P-P) (P-P = *o*-MeO-dppe, **3b**; *o*-MeO-dppp, **4b**) occurred at room temperature. The most relevant $^{31}P\{^{1}H\}$ and ^{1}H NMR chemical shifts and coupling constants for **3b** and **4b** are reported in Tables 2 and 3, respectively. The excess CO was released and nitrogen was gently bubbled through the solution previously cooled to –30 °C for 2 min to eliminate any trace of CO. Both complexes were found to be stable also in the absence of CO. Unlike **3b**, **4b** was generated even by bubbling CO through **4a** solutions for 5 min at room temperature. A procedure analogous to that described above was applied to prepare CH_2Cl_2 solutions of **3b** and **4b** for the IR characterization: ν(C=O) 1669 (**3b**), 1674 (**4b**) cm^{-1}.

In Situ Synthesis of the β-Keto Chelates [Pd(CH_2CH_2C(O)Me)-(P-P)]BAr'_4: In a typical experiment, a solution of PdCl(COMe)-(P-P) (0.03 mmol) in CD_2Cl_2 (2 mL) was prepared as above in a Schlenk tube at –30 °C under nitrogen. Ethene was bubbled through the solution maintained at –30 °C for 2 min and then a solid sample of $NaBAr'_4$ (0.03 mmol) was added to the solution to scavenge the chloride ligand from Pd. The resulting solution was transferred into a 10-mm sapphire tube. $^{31}P\{^{1}H\}$ and ^{1}H NMR spectra were acquired in the temperature range from 20 to –90 °C. Irrespective of the diphosphane ligand, the $^{31}P\{^{1}H\}$ and ^{1}H NMR spectra of this sample showed the quantitative conversion of the (acyl)chloride complex into the corresponding β-chelate complex [Pd(CH_2CH_2C(O)Me)(P-P)]BAr'_4 (P-P = *o*-MeO-dppe, **3c**; *o*-MeO-dppp, **4c**). IR spectra of **3c** and **4c** were acquired from CH_2Cl_2 solutions of these compounds prepared by applying the same synthetic protocol as described above, using CH_2Cl_2 instead of CD_2Cl_2. The IR values of the CO stretching frequencies are reported in Table 4.

3c: $^{31}P\{^{1}H\}$ NMR (161.98 MHz, CD_2Cl_2, –70 °C): δ = 57.36 (d, $^{2}J_{P,P}$ = 26.9 Hz, P_A), 25.43 (br., P_M) ppm. ^{1}H NMR (400.13 MHz, CD_2Cl_2, –70 °C): δ = 0.82 (m, 1 H, PdCH*H*), 1.21 (m, 1 H, PdC*H*H), 2.05 (m, 2 H, PCH_2), 2.42 (m, 3 H, COMe), 2.58 (m, 2 H, P′CH_2), 2.80 (m, 1 H, COCH*H*), 3.08 (m, 4 H, COC*H*H + OMe), 3.51 (s, 3 H, OMe), 3.80 (s, 3 H, OMe), 3.83 (s, 3 H, OMe), 6.72–7.82 (m, 27 H, Ar), 8.48 [dd, $^{2}J_{H,P}$ = 17.0 Hz, $^{3}J_{H,H}$ = 7.3 Hz, 1 H, *o*-H-$Ar_{ax.}$(A)] ppm.

4c: $^{31}P\{^{1}H\}$ NMR (161.98 MHz, CD_2Cl_2, –70 °C): δ = 33.51 (d, $^{2}J_{PP}$ = 57.9 Hz, P_A), –12.4 (br., P_M) ppm. ^{1}H NMR (400.13 MHz, CD_2Cl_2, –70 °C): δ = 0.95 (m, 2 H, $PdCH_2$), 2.21 (s, 3 H, COMe), 2.31 (m, 3 H, PC*H*H + CH_2), 2.51 (m, 2 H, PCH*H* + P′CH*H*), 2.92 (m, 3 H, $COCH_2$ + P′C*H*H), 3.59 (s, 3 H, OMe), 3.70 (s, 3 H, OMe), 3.83 (s, 3 H, OMe), 3.86 (s, 3 H, OMe), 6.62–7.83 (m, 27 H, Ar), 8.28 [dd, $^{2}J_{H,P}$ = 17.0 Hz, $^{3}J_{H,H}$ = 7.1 Hz, 1 H, *o*-H-$Ar_{ax.}$(A)] ppm.

In Situ Generation and Migratory Insertion Barriers of [PdMe(CO)-(P-P)]BAr'_4. HPNMR Experiments: In a typical experiment, the methyl-chlorido complex [PdCl(Me)(P-P)] (0.03 mmol) was dissolved in deoxygenated CD_2Cl_2 (2 mL) and the resulting solution was then transferred into a 10-mm sapphire tube, which was cooled to –120 °C by means of an ethanol/liquid nitrogen bath. CO was bubbled through this solution for 2 min at this temperature, fol-

lowed by the addition of $NaBAr'_4$ (0.03 mmol). The CO pressure was adjusted to the desired value (5–20 bar). The solution was shaken for 2 min at –120 °C, followed by the introduction of the sapphire tube into the probe-head previously cooled to –90 °C. Irrespective of the diphosphane ligand, the $^{31}P\{^1H\}$ and ^1H NMR spectra showed the quantitative conversion of the starting methyl-chlorido complex into the corresponding carbonyl-methyl complexes [PdMe(CO)(P-P)]BAr'_4 (P-P = *o*-MeO-dppe, **3d**; *o*-MeO-dppp, **4d**) (selected $^{31}P\{^1H\}$ and ^1H NMR spectroscopic data of the carbonyl-methyl complexes are reported in Tables 5 and 6, respectively). Afterwards the probe temperature was gradually increased and $^{31}P\{^1H\}$ and ^1H NMR spectra were recorded at each intermediate temperature. Increasing the temperature converted each carbonyl-methyl complex into the corresponding (acetyl)carbonyl derivative [Pd(COMe)(CO)(P-P)]BAr'_4 (P-P = *o*-MeO-dppe, **3e**; *o*-MeO-dppp, **4e**) (selected $^{31}P\{^1H\}$ and ^1H NMR spectroscopic data of the (acetyl)carbonyl complexes are reported in Tables 5 and 6, respectively). At the conversion temperature, the decrease in concentration of the carbonyl-methyl complex was followed by $^{31}P\{^1H\}$ NMR spectroscopy. Spectra were taken at intervals of 5–10 min, depending on conditions. The reaction was followed for 2–3 half-lives. IR spectra of **3e** and **4e** were acquired from CH_2Cl_2 solutions of these compounds prepared by applying the same synthetic protocol as described above, using CH_2Cl_2 instead of CD_2Cl_2. The IR values of the CO stretching frequencies are reported in Table 4.

Carbonylation of the β-Keto Chelates [Pd($CH_2CH_2C(O)Me$)(P-P)]BAr'_4. HPNMR Experiments: CD_2Cl_2 (2 mL) solutions of the β-keto chelates [Pd($CH_2CH_2C(O)Me$)(P-P)]BAr'_4 (P-P = *o*-MeO-dppe, **3c**; *o*-MeO-dppp, **4c**) (0.03 mmol) were synthesized in situ in a Schlenk tube at –30 °C, as described above. Nitrogen was bubbled through the solution to eliminate any trace of ethene. The solutions were transferred into a 10-mm sapphire tube at room temperature. Then the sapphire tube was introduced in a pre-cooled NMR probe (–90 °C) and $^{31}P\{^1H\}$ and ^1H NMR spectra were acquired at this temperature. The sapphire tube was then removed from the probe and immersed in an ethanol/liquid nitrogen thermostat bath (ca. –120 °C) before to be charged with CO (5–20 bar). Afterwards the sapphire tube was introduced again into the NMR probe head at –90 °C. $^{31}P\{^1H\}$ and ^1H NMR spectra showed that the β-chelate complexes were still present. Afterwards the probe temperature was gradually increased and $^{31}P\{^1H\}$ and ^1H NMR spectra were recorded at each intermediate temperature. Increasing the temperature caused the conversion of the β-chelate complex into the corresponding (acyl)carbonyl derivative [Pd(CO)($COCH_2CH_2C(O)Me$)(P-P)]BAr'_4 (P-P = *o*-MeO-dppe, **3g**; *o*-MeO-dppp, **4g**) via the (alkyl)carbonyl complexes [Pd(CO)($CH_2CH_2C(O)Me$)(P-P)]BAr'_4 (P-P = *o*-MeO-dppe, **3f**; *o*-MeO-dppp, **4f**). Selected high-pressure $^{31}P\{^1H\}$ NMR spectra of the carbonylation of either **3c** or **4c** under 20 bar of CO are shown in Figures 2 and 3, respectively. Selected $^{31}P\{^1H\}$ and ^1H NMR spectroscopic data of the complexes **3f**, **4f**, **3g**, and **4g** are reported in Tables 2 and 3, respectively. At the conversion temperature the decrease in concentration of the β-keto chelates was followed by $^{31}P\{^1H\}$ NMR spectroscopy. Spectra were taken at intervals of 5–10 min, depending on conditions. The reaction was followed for 2–3 half-lives.

[Pd($CH_2CH_2C(O)Me$)(P-P)]BAr'_4/[Pd($COCH_2CH_2C(O)Me$)(CO)(P-P)]BAr'_4 Equilibria: Solutions of the (acyl)carbonyl complexes **3g** and **4g**, prepared as reported above in HPNMR tubes, were immersed in a thermostat bath at –20 °C. CO was released and then couples of vacuum-nitrogen cycles were applied. $^{31}P\{^1H\}$ and ^1H NMR spectra of these samples acquired at –20 °C allowed us to follow the transformation of the (acyl)carbonyl complexes into the corresponding β-chelates **3c** and **4c**.

Catalytic Copolymerization Reactions in CH_2Cl_2: CH_2Cl_2 (75 mL), saturated with CO at room temperature, was introduced by suction into an autoclave (250 mL), previously evacuated by a vacuum pump, containing the catalyst precursor (0.010 mmol) and $NaBAr'_4$ (0.012 mmol). The autoclave was charged with the required pressures of CO and C_2H_4 at room temperature and then heated. As soon as the temperature reached 50 °C, stirring (1200 rpm) was started and the catalytic reaction was conducted under constant pressure. After 20 min, the autoclave was cooled by means of an ice-water bath and the unreacted gases were released. The insoluble copolymer was filtered off, washed with CH_2Cl_2, and dried under vacuum at 60 °C to constant weight.

Catalytic Copolymerization Reactions in MeOH: Typically, MeOH (100 mL), was introduced by suction into an autoclave (250 mL), previously evacuated by a vacuum pump, containing the catalyst precursor (0.0024 mmol) and 1,4-benzoquinone (BQ, 0.192 mmol). The autoclave was charged with the desired pressure of CO and C_2H_4 at room temperature and then heated. As soon as the temperature reached 85 °C, stirring (1200 rpm) was started and the catalytic reaction was conducted under constant pressure for 1 h. Afterwards the autoclave was cooled by means of an ice-water bath and the unreacted gases were released. The insoluble copolymer was filtered off, washed with MeOH, and dried under vacuum at 60 °C to constant weight.

Crystal Structure Determination of 3a·$CHCl_3$: Several crystallization attempts with different solvents were performed and only the diffusion of toluene into a $CHCl_3$ solution of **3a** gave a single crystal, although of poor quality. Crystal data and structure refinement details for **3a·$CHCl_3$** are reported in Table 9.

Table 9. Crystal data and structure refinement details for **3a·$CHCl_3$**.

Empirical formula	$C_{32}H_{36}Cl_4O_4P_2Pd$
Molecular mass [g mol^{-1}]	794.75
Crystal color, shape	white, plate
Crystal size [mm]	$0.20 \times 0.10 \times 0.05$
Temperature [K]	223
Crystal system	monoclinic
Space group	$P2_1/c$
a [Å]	9.294(6)
b [Å]	23.054(10)
c [Å]	22.295(11)
β [°]	94.75(5)
V [Å^3]	4761(4)
Z	4
Density (calculated) [g cm^{-3}]	1.109
F(000)	1616
θ range [°]	3.98–23.27
Radiation wavelength [Å]	Mo-K_α/0.71073
Absorption coefficient [mm^{-1}]	0.707
Reflections collected	18877
Independent reflections	6802
Data/restraints/parameters	5200/0/390
Gof on F^2	1.111
*R*1, *wR*2 [$I > 2\sigma(I)$]	0.1038, 0.2801
*R*1, *wR*2 (all data)	0.1190, 0.2970
Largest diff. peak/hole [e Å^{-3}]	1.915/–2.054

X-ray diffraction intensity data were collected at 223 K with an Oxford Diffraction CCD diffractometer with graphite-monochromated Mo-K_α radiation (λ = 0.71073 Å) using ω-scans. Cell refinement, data reduction, and empirical absorption correction were

carried out with the Oxford diffraction software and SADABS.[12a] All structure determination calculations were performed with the WINGX package[12b] with SIR-97,[12c] SHELXL-97,[12d] and ORTEP-3 programs.[12e] Final refinements based on F^2 were carried out with anisotropic thermal parameters for all non-hydrogen atoms, which were included using a riding model with isotropic U values depending on the U_{eq} of the adjacent carbon atoms.

CCDC-632065 contains the supplementary crystallographic data for this paper. These data can be obtained free of charge from The Cambridge Crystallographic Data Centre via www.ccdc.cam.ac.uk/data_request/cif.

Acknowledgments

Thanks are due to the European Commission for financing the following projects: PALLADIUM (RTN contract no. HPRN-CT-2002-00196), IDECAT (NoE contract no. NMP3-CT-2005-011730), and NANOHYBRID (STREP contract no. NMP3-CT-2005-516972).

[1] a) E. Drent, P. H. M. Budzelaar, *Chem. Rev.* **1996**, *96*, 663–681; b) C. Bianchini, A. Meli, *Coord. Chem. Rev.* **2002**, *225*, 35–66.

[2] a) J. Schwarz, E. Herdtweck, W. A. Herrmann, M. G. Gardiner, *Organometallics* **2000**, *19*, 3154–3160; b) C. Bianchini, H. M. Lee, A. Meli, W. Oberhauser, M. Peruzzini, F. Vizza, *Organometallics* **2002**, *21*, 16–33; c) C. Bianchini, A. Meli, G. Müller, W. Oberhauser, E. Passaglia, *Organometallics* **2002**, *21*, 4965–4977; d) C. Bianchini, A. Meli, W. Oberhauser, A. M. Segarra, C. Claver, E. J. Garcia Suarez, *J. Mol. Catal. A: Chemical* **2006**, in press; e) M. A. Zuideveld, P. C. J. Kamer, P. W. N. M. van Leeuwen, P. A. A. Klusener, H. A. Stil, C. F. Roobeek, *J. Am. Chem. Soc.* **1998**, *120*, 7977–7978.

[3] a) G. Vespui, F. Schanssema, A. R. Sheldon, *Angew. Chem. Int. Ed.* **2000**, *39*, 804–806; b) E. Drent, W. P. Mul, A. A. Smaardijk, "Polyketones" in *Encyclopedia of Polymer Science and Technology*, 3rd ed., Wiley-Interscience, New York, **2002**; c) W. P. Mul, E. Drent, P. Jansens, A. H. Kramer, N. H. W. Sonnemans, *J. Am. Chem. Soc.* **2001**, *123*, 5350–5351; d) W. P. Mul, H. Dirkzwager, A. A. Broekhuis, H. J. Heeres, A. J. van der Linden, A. Guy Orpen, *Inorg. Chim. Acta* **2002**, *327*, 147–159, and refs therein.

[4] I. M. Angulo, E. Bouwman, R. van Gorkum, S. M. Lok, M. Lutz, A. L. Spek, *J. Mol. Catal. A* **2003**, *202*, 97–106.

[5] a) I. M. Angulo, E. Bouwman, M. Lutz, W. P. Mul, A. L. Spek, *Inorg. Chem.* **2001**, *40*, 2073–2082; b) K. R. Dunbar, J.-S. Sun, A. Quillevèrè, *Inorg. Chem.* **1994**, *33*, 3598–3601; c) C. Bianchini, A. Meli, W. Oberhauser, *Dalton Trans.* **2003**, 2627–2635.

[6] I. M. Angulo, E. Bouwman, S. M. Lok, M. Lutz, W. P. Mul, A. L. Spek, *Eur. J. Inorg. Chem.* **2001**, 1465–1473.

[7] a) P. Braunstein, J. Durand, M. Knorr, C. Strohmann, *Chem. Commun.* **2001**, 211–212; b) W. P. Mul, H. Oosterbeek, G. A. Beitel, G. J. Kramer, E. Drent, *Angew. Chem. Int. Ed.* **2000**, *39*, 1848–1851; c) J. Liu, B. T. Heaton, J. A. Iggo, R. Whyman, J. F. Bickley, A. Steiner, *Chem. Eur. J.* **2006**, *12*, 4417–4430; d) P. Braunstein, C. Frison, X. Morise, *Angew. Chem. Int. Ed.* **2000**, *39*, 2867–2870; e) J. Liu, B. T. Heaton, J. A. Iggo, R. Whyman, *Angew. Chem. Int. Ed.* **2004**, *43*, 90–94; f) K. Nozaki, N. Sato, Y. Tonomura, M. Yasutomi, H. Takaya, T. Hiyama, T. Matsubara, N. Koga, *J. Am. Chem. Soc.* **1997**, *119*, 12779–12795; g) F. C. Rix, M. Brookhart, P. S. White, *J. Am. Chem. Soc.* **1996**, *118*, 4746–4764.

[8] L. Toniolo, S. M. Kulkarni, D. Fatutto, R. V. Chaudhari, *Ind. Eng. Chem. Res.* **2001**, *40*, 2037–2045.

[9] R. E. Rülke, J. M. Ernsting, A. L. Spek, C. J. Elsevier, P. W. N. M. van Leeuwen, K. Vrieze, *Inorg. Chem.* **1993**, *32*, 5769–5778.

[10] M. Brookhart, B. Grant, A. F. Volpe, *Organometallics* **1992**, *11*, 3920–3922.

[11] C. Bianchini, A. Meli, A. Traversi, Ital. Pat. FI A,000,025, **1997**.

[12] a) G. M. Sheldrick, *SADABS*, Program for empirical absorption corrections, University of Göttingen, Göttingen, Germany, **1986**; b) L. J. Farrugia, *J. Appl. Crystallogr.* **1999**, *32*, 837–838; c) A. Altomare, M. C. Burla, M. Cavalli, G. L. Cascarano, C. Giacovazzo, A. Gagliardi, G. G. Moliterni, G. Polidori, R. Spagna, *J. Appl. Crystallogr.* **1999**, *32*, 115–119; d) G. M. Sheldrick, *SHELX-97*, University of Göttingen, Germany, **1997**; e) M. N. Burnett, C. K. Johnson, *ORTEP-3*, Report ORNL-6895, Oak Ridge National Laboratory, Oak Ridge, TN, **1996**.

Received: December 29, 2006
Published Online: April 18, 2007

